Integral Sliding Mode Control: Performance, Modification, and Improvement

Yongping Pan, *Member, IEEE*, Chenguang Yang, *Senior Member, IEEE*, Lin Pan, and Haoyong Yu, *Member, IEEE*

***Abstract*—Sliding mode control (SMC) is attractive for nonlinear systems due to its invariance for both parametric and nonparametric uncertainties. However, the invariance of SMC is not guaranteed in a reaching phase. Integral SMC (ISMC) eliminates the reaching phase such that the invariance is achieved in an entire system response. To reduce chattering in ISMC, it was suggested that the switching element is smoothed by using a low-pass filter and an integral sliding variable is modified. This study discusses several crucial problems regarding the performance, modification, and improvement of ISMC. First, the modification of the integral sliding variable is revealed to be unnecessary as it degrades the performance of a sliding phase; second, ISMC is shown to be a kind of global SMC; third, it is manifested that a high-order ISMC design with super twisting involves a stability condition that may be infeasible in theory; finally, an efficient solution is suggested to attenuate chattering in ISMC without the degradation of tracking accuracy and the solution is extended to the case with uncertain control gain functions. Comprehensive simulation results have verified the arguments of this study.**

***Index Terms*—Chattering attenuation, disturbance rejection, integral sliding mode, high-order sliding mode, nonlinear system, uncertainty estimation.**

I. Introduction

SLIDING mode control (SMC) is a variable structure control technique which applies a switching control law to alter the plant dynamics such that the plant states slide along a cross section termed sliding surface of its normal behavior. SMC has attracted widespread applications in industrial informatics, e.g., see [1]–[9]. An SMC process usually has two phases, namely a reaching phase and a sliding phase [10]. In the *reaching phase*, the plant states are forced to reach a prespecified sliding surface in finite time. Once the plant states reach the sliding surface, the closed-loop system is adaptively altered to a sliding mode such that the plant states slide toward the origin along the sliding surface. This duration is called the *sliding phase*. In the sliding phase, the system response remains invariant for both parametric and nonparametric uncertainties [11]. However, during the reaching phase, the invariance of SMC is not guaranteed and the system response is sensitive to perturbations [12].

Integral SMC (ISMC) eliminates the reaching phase by enforcing the sliding mode in an entire system response so that the invariance of SMC is ensured from the initial time instant [13]. The imperfect implementation of high-frequency switching in SMC results in chattering at control responses [14]. To reduce chattering in ISMC, the switching element is smoothed by using a low-pass filter based on the equivalent control method, and an integral sliding variable is modified for facilitating stability analysis in [13]. The approach of [13] was applied to position control of robot manipulators and load pressure control of die-cushion cylinder drives in [15] and [16], respectively. A more popular way to attenuate chattering in ISMC is to integrate with high-order SMC [17]–[23]. In high-order ISMC, the switching element appears in a time derivative of the sliding variable such that the actual control law is smoothed by an integral [24].

In this study, several crucial issues regarding the performance and modification of ISMC are discussed and an efficient solution is finally suggested to improve the performance of ISMC. First, the modification of the integral sliding variable is demonstrated to be unnecessary; second, ISMC and global SMC (GSMC) are shown to be closely connected; third, the stability condition of a high-order ISMC design with super twisting is proven to be theoretically infeasible; finally, a simple and feasible solution is suggested to reduce chattering in ISMC without the degradation of tracking accuracy. Simulations are provided throughout the study to validate the arguments.

Throughout this paper, $\mathbb{R}$, $\mathbb{R}^+$, and $\mathbb{R}^n$ are the spaces of real numbers, positive real numbers, and real n-vectors, respectively, $\|\boldsymbol{x}\|$ is the Euclidean norm of $\mathbf{x}$, $\Omega_c := \{\boldsymbol{x} | \|\boldsymbol{x}\| \leq c\}$ is the ball of radius c, and $\mathrm{sgn}(x)$ is the standard signum function, where $c \in \mathbb{R}^+$, $x \in \mathbb{R}$, $\boldsymbol{x} \in \mathbb{R}^n$, and n is a natural number. For the sake of brevity, in the following sections, the arguments of a function may be omitted while the context is sufficiently explicit.

II. Integral SMC

This section presents the ISMC design in [13]. For the simplification of illustration, consider a class of perturbed uncertain

Manuscript received July 19, 2017; revised September 1, 2017; accepted October 2, 2017. Date of publication October 11, 2017; date of current version July 2, 2018. This work was supported in part by the FRC Tier 1, Faculty of Engineering, National University of Singapore, Singapore, under WBS R397000218112 and in part by the BMRC, Agency for Science, Technology and Research (A*STAR), Singapore under Grant 15/12124019. Paper no. TII-17-2068. *(Corresponding author: H. Yu).*

Y. Pan and H. Yu are with the Department of Biomedical Engineering, National University of Singapore, Singapore 117583 (e-mail: biepany@nus.edu.sg; bieyhy@nus.edu.sg).

C. Yang is with the Zienkiewicz Centre for Computational Engineering, Swansea University, Swansea SA1 8EN, U.K. (e-mail: cyang@ieee.org).

L. Pan is with the School of Logistics Engineering, Wuhan University of Technology, Wuhan 430070, China (e-mail: lin.pan@whut.edu.cn).

Color versions of one or more of the figures in this paper are available online at http://ieeexplore.ieee.org.

Digital Object Identifier 10.1109/TII.2017.2761389

affine-in-control nonlinear systems [18]

$$\begin{cases} \dot{x}_i = x_{i+1} \ (i = 1, 2, \ldots, n-1) \\ \dot{x}_n = f(\boldsymbol{x}) + g(\boldsymbol{x})u + d(t) \end{cases} \tag{1}$$

where $\boldsymbol{x}(t) = [x_1(t), x_2(t), \ldots, x_n(t)]^T \in \mathbb{R}^n$ is a state vector, $f : \mathbb{R}^n \mapsto \mathbb{R}$ is a nonlinear drifting function, $g : \mathbb{R}^n \mapsto \mathbb{R}$ is a control gain function, $u(t) \in \mathbb{R}$ is a control input, and $d(t) \in \mathbb{R}$ presents a unknown perturbation caused by *nonparametric uncertainties* such as unmodeled dynamics and external disturbances. In addition, f and g are separated into

$$f(\boldsymbol{x}) = f_0(\boldsymbol{x}) + \Delta f(\boldsymbol{x}) \tag{2}$$

$$g(\boldsymbol{x}) = g_0(\boldsymbol{x}) + \Delta g(\boldsymbol{x}) \tag{3}$$

where $f_0, g_0 : \mathbb{R}^n \mapsto \mathbb{R}$ are nominal parts, and $\Delta f, \Delta g : \mathbb{R}^n \mapsto \mathbb{R}$ are perturbed parts caused by *parametric uncertainties* such as inaccurate parameters and parameter variations.[1] Let $x_d(t) \in \mathbb{R}$ be a desired output. The following standard assumptions of SMC are introduced for the subsequent discussions.

Assumption 1: Δf are Δg are locally bounded and $g \neq 0$, i.e., there exist some constants $\bar{f}, \underline{g}, \bar{g} \in \mathbb{R}^+$ such that $|\Delta f| \leq \bar{f}$, $|\Delta g| \leq \bar{g}$ and $|g| > \underline{g}\ \forall \boldsymbol{x} \in \Omega_{c_x} \subset \mathbb{R}^n$ with $c_x \in \mathbb{R}^+$. Without loss of generality, it is assumed that $g > 0$.

Assumption 2: d is globally bounded, such that there exists a constant $\bar{d} \in \mathbb{R}^+$ to satisfy $|d(t)| \leq \bar{d}\ \forall t \geq 0$.

Assumption 3: $x_d^{(i)}$ exist and are bounded for $i = 0$ to n.

For clear illustration, the case of $\Delta g = 0$ is initially considered, and the extension to the case of $\Delta g \neq 0$ will be presented in Section VI. Let $\boldsymbol{x}_d(t) := [x_d(t), \dot{x}_d(t), \cdots, x_d^{(n-1)}(t)]^T$ and define the tracking error $\boldsymbol{e}(t) := \boldsymbol{x}(t) - \boldsymbol{x}_d(t) = [e_1(t), e_2(t), \ldots, e_n(t)]^T$, where $e_1(t) := x_1(t) - x_d(t)$. Then, one gets the open-loop tracking error dynamics

$$\begin{cases} \dot{e}_i = e_{i+1} \ (i = 1, 2, \cdots, n-1) \\ \dot{e}_n = [f_0(\boldsymbol{x}) - x_d^{(n)}] + g_0(\boldsymbol{x})u + h(\boldsymbol{x}, t) \end{cases} \tag{4}$$

with $h : \mathbb{R}^n \times \mathbb{R}^+ \mapsto \mathbb{R}$ a lumped perturbation given by

$$h(\boldsymbol{x}, t) := \Delta f(\boldsymbol{x}) + d(t). \tag{5}$$

The conventional sliding variable $s_0 \in \mathbb{R}$ is given by $s_0(\boldsymbol{e}) = (d/dt + \lambda)^{n-1} e_1$ [28], in which $\lambda \in \mathbb{R}^+$ is a design parameter specifying the performance during the sliding phase.[2] It follows from the definitions of e_1 and $\boldsymbol{e}$ that[2]

$$s_0(\boldsymbol{e}) = [\Lambda^T \ 1]\boldsymbol{e} \tag{6}$$

with $\Lambda := [\lambda^{(n-1)}, (n-1)\lambda^{(n-2)}, \cdots, (n-1)\lambda]^T$. Taking the time derivative of s_0 in (6) and using (4), one obtains

$$\dot{s}_0 = [f_0(\boldsymbol{x}) + v(\boldsymbol{x}, t)] + g_0(\boldsymbol{x})u + h(\boldsymbol{x}, t) \tag{7}$$

where $v(\boldsymbol{x}, t) := [0 \ \Lambda^T]\boldsymbol{e}(t) - x_d^{(n)}(t)$. For the reduced-order system (7), choose the following control law:

$$u(t) = u_0(t) + u_1(t) \tag{8}$$

where $u_0(t) \in \mathbb{R}$ is a nominal control for (7), and $u_1(t) \in \mathbb{R}$ is a discontinuous control for the rejection of h. Letting $h = 0$ and $u = u_0$ in (7) and choosing

$$u_0 = -[k_c s_0 + f_0(\boldsymbol{x}) + v(\boldsymbol{x}, t)]/g_0(\boldsymbol{x}) \tag{9}$$

leads to the ideal closed-loop dynamics

$$\dot{s}_0 + k_c s_0 = 0 \tag{10}$$

where $k_c \in \mathbb{R}^+$ is a control gain parameter.

The following ISMC design follows [13]. A systemical description of the method of [13] can be found in [14]. According to the equivalent control method [25, Sec. 2], an integral sliding variable is designed as follows:

$$s(t) = s_0(\boldsymbol{e}) + z(t) \tag{11}$$

where $z(t) \in \mathbb{R}$ is an integral term given by

$$\dot{z} = -\frac{\partial s_0}{\partial \boldsymbol{e}} \begin{bmatrix} \bar{\boldsymbol{e}}_1 \\ [f_0(\boldsymbol{x}) - x_d^{(n)}] + g_0(\boldsymbol{x})u_0 \end{bmatrix} \tag{12}$$

with $\bar{\boldsymbol{e}}_1 := [e_2, e_3, \ldots, e_n]^T$ and $z(0) = -s_0(\boldsymbol{e}(0))$ such that $s(0) = 0$. Applying the expressions of s_0 in (6), u_0 in (9) and v under (7) to (12), one obtains

$$\dot{z} = -[\Lambda^T \ 1] \begin{bmatrix} \bar{\boldsymbol{e}}_1 \\ -k_c s_0 - [0 \ \Lambda^T]\boldsymbol{e} \end{bmatrix} = k_c s_0.$$

Thus, the integral sliding variable s in (11) becomes[3]

$$s(t) = s_0(\boldsymbol{e}(t)) - s_0(\boldsymbol{e}(0)) + k_c \int_0^t s_0(\boldsymbol{e}(\tau))d\tau. \tag{13}$$

Taking the time derivative of s in (13) and using (7) yields

$$\dot{s} = [f_0(\boldsymbol{x}) + v(\boldsymbol{x}, t)] + g_0(\boldsymbol{x})u + h(\boldsymbol{x}, t) + k_c s_0.$$

Applying (8) with (9) to the above result, one obtains

$$\dot{s} = g_0(\boldsymbol{x})u_1 + h(\boldsymbol{x}, t). \tag{14}$$

Now, choose the discontinuous control

$$u_1 = -\alpha \mathrm{sgn}(s), \ \alpha \geq (\bar{f} + \bar{d} + \eta)/g_0 \tag{15}$$

in which $\eta \in \mathbb{R}^+$ is a constant specifying the converging rate of s. Substituting (15) into (14), one obtains

$$\begin{aligned} s\dot{s} &= s\big(h(\boldsymbol{x}, t) - g_0(\boldsymbol{x})\alpha \mathrm{sgn}(s)\big) \\ &\leq sh(\boldsymbol{x}, t) - (\bar{f} + \bar{d} + \eta)|s| \\ &\leq (|h(\boldsymbol{x}, t)| - \bar{f} - \bar{d} - \eta)|s|. \end{aligned}$$

Applying (5) with Assumptions 1 and 2 to the above result, one gets a standard reaching law

$$s\dot{s} \leq -\eta|s| \qquad \forall \boldsymbol{x} \in \Omega_{c_x} \tag{16}$$

implying $s(t) \to 0$ in finite time. The setting $s(0) = 0$ removes the reaching time resulting in $s(t) = 0\ \forall t \geq 0$. Once the plant

[1] The extension to the case that Δf and Δg explicitly depend on time t, i.e., $\Delta g(\boldsymbol{x}, t)$ and $\Delta f(\boldsymbol{x}, t)$, can be referred to [27, Remark 1].

[2] The mapping $s_0 : \mathbb{R}^n \mapsto \mathbb{R}$ is also called a switching function [14].

[3] A so-called total SMC of [29] is exactly the same as the ISMC of [13] where they share the same sliding variable s given by (13).

states are confined to the sliding manifold $s = 0$, the equivalent control $u_{1\text{eq}}$ is obtained by setting $\dot{s} = 0$ in (14) as follows:

$$u_{1\text{eq}} = -h(\boldsymbol{x}, t)/g_0(\boldsymbol{x}). \tag{17}$$

Applying $u = u_0 + u_{1\text{eq}}$ with u_0 in (9) and $u_{1\text{eq}}$ in (17) to (7), one gets a motion equation in the sliding mode identical to the ideal dynamics (10) so that $s_0 \to 0$ exponentially implying $\boldsymbol{e} \to \mathbf{0}$ exponentially. Therefore, the nominal control u_0 achieves the ideal dynamics (10) as if the perturbation h in (7) does not exist. Let $\hat{h}(t) \in \mathbb{R}$ be an estimate of h given by

$$\hat{h} = -g_0(\boldsymbol{x})u_1. \tag{18}$$

To illustrate the performance of the above ISMC, consider a simplified model of underwater vehicles [28, Sec. 7]

$$\begin{cases} \dot{x}_1 = x_2 \\ \dot{x}_2 = -cx_2|x_2|/m + (1/m)u + d(t) \end{cases} \tag{19}$$

where x_1 (m) is the vehicle position, u (N) is the control force, m (kg) is the vehicle mass, and c is a drag coefficient. Note that m and c are not exactly known in practice. For simulations, let $\boldsymbol{x}(0) = [-1, 0]^T$, $m = m_0$, $c = c_0 + 0.2\sin(|x_2|t)$, and $d(t) = 3\sin(\pi t)$, where $m_0 = 3$ and $c_0 = 1.2$ are nominal values of m and c, respectively. The desired trajectory is comprised of an acceleration $\ddot{x}_d = 2$ m/s^2 at $t \in [0, 2)$ s, a velocity $\dot{x}_d = 4$ m/s at $t \in [2, 4)$ s, and an acceleration $\ddot{x}_d = -2$ m/s^2 at $t \in [4, 6)$ s [28, Sec. 7]. To construct the ISMC in (8), set $f_0 = 1.2\, x_2|x_2|/3$, $g_0 = 1/3$, and $k_c = 5$ for u_0 in (9), $\lambda = 5$ and $s_0(\boldsymbol{e}(0)) = [\lambda, 1]\boldsymbol{e}(0) = -5$ for s in (13), and $\alpha = 13$ for u_1 in (15).

Simulations are carried out in MATLAB software, where the solver is set to be fixed-step ODE 4, the step size is set to be 0.1 ms, and the other settings are kept at their defaults. Simulation trajectories are given in Fig. 1, where the state vector $\boldsymbol{x}$ exactly tracks the desired output $\boldsymbol{x}_d$ under a control input u with serious chattering after a short transient process, the estimate $\hat{h}$ does not follows the perturbation h, the sliding variable s keeps very near to 0 from $t = 0$, but its time derivative $\dot{s}$ exhibits chattering with low amplitudes due to imperfect switches caused by the digital simulation with a sampling time.

Remark 1: The system (1) under the ISMC law $u = u_0 + u_1$ in (8) with u_0 in (9), u_1 in (15), and s in (13) obtains exponential convergence of the tracking error $\boldsymbol{e}$ to $\mathbf{0}$, in which the reaching phase is eliminated resulting in the invariance throughout an entire system response. However, the above ISMC design includes two major limitations: 1) Chattering of the conventional SMC is inherited resulting in difficulty for practical applications; and 2) the estimation of the perturbation h by $\hat{h}$ in (18) is not realizable due to the intrinsic discontinuity of u_1.

Remark 2: Like most existing SMC results, we assume that the state vector $\boldsymbol{x}$ in the system (1) is fully measurable. If only x_1 is measurable, x_2 to x_n can be exactly estimated by sliding mode observers (SMOs). For instance, the following SMO can be applied to the system (19) [10, Sec. 1.6]:

$$\begin{cases} \dot{\hat{x}}_1 = -\beta\text{sgn}(z_1) \\ \tau\dot{\hat{x}}_2 = \varphi(\hat{x}_2, u) - \hat{x}_2 - \beta\text{sgn}(z_1) \end{cases} \tag{20}$$

in which $\varphi(\hat{x}_2, u) := -c_0\hat{x}_2|\hat{x}_2|/m + (1/m_0)u$ is the nominal part of the system (19), $\hat{x}_1 \in \mathbb{R}$ and $\hat{x}_2 \in \mathbb{R}$ denote estimates of

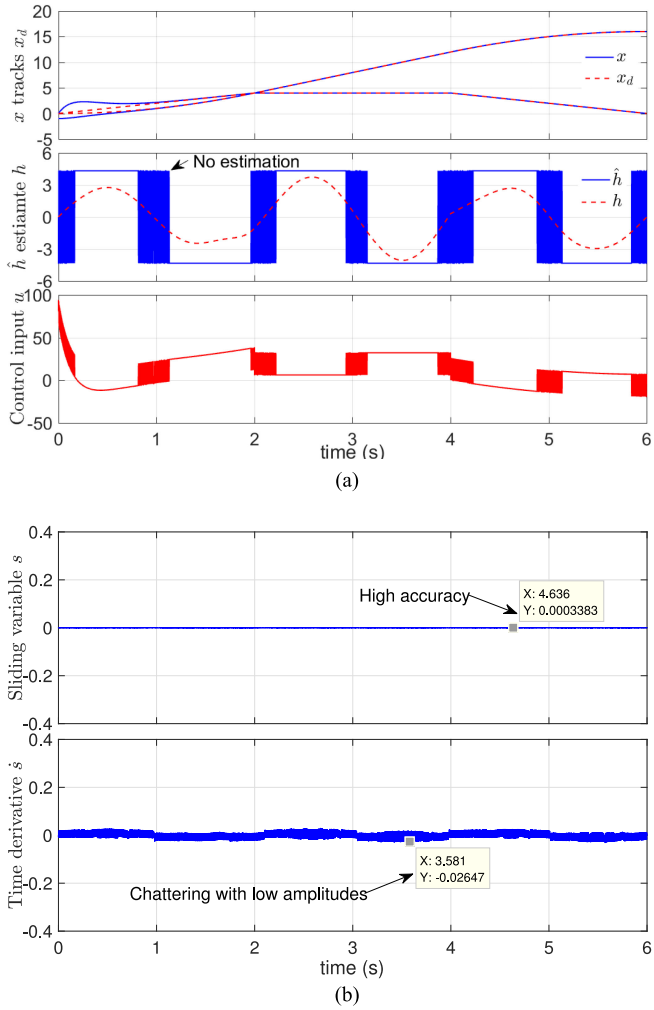

Fig. 1. Simulation trajectories by the original ISMC in Section II. (a) Control and estimation performances. (b) Evaluations of s and $\dot{s}$.

x_1 and x_2, respectively, $z_1 := \hat{x}_1 - x_1$ is an estimation error, $\beta \in \mathbb{R}^+$ is a switching gain, and $\tau \in \mathbb{R}^+$ is a filtering constant. Control results under the SMO (20) with $\beta = 4.5$ and $\tau = 0.01$ are depicted in Fig. 2 . It is shown that the SMO (20) provides a favorable estimation of x_2 and the tracking accuracy of the SMO-based ISMC is just slightly degraded compared with that of the original ISMC. Please refer to [10] for more about SMOs as they are out of the scope of this discussion.

III. Integral Sliding Surface Modification

To reduce chattering in the ISMC design of Section II, it was suggested in [14, Sec. 7] that the discontinuous control u_1 given by (15) is low-pass filtered by a first-order linear filter

$$\mu\dot{u}_{1\text{av}}(t) = -u_{1\text{av}}(t) + u_1(t) \tag{21}$$

with $u_{1av}(0) = 0$, where $u_{1\text{av}}(t) \in \mathbb{R}$ is an averaging counterpart of $u_1(t)$, and $\mu \in (0, 1)$ is a filtering constant that should be small enough to avoid disturbing the slow component of the switching action in u_1 equal to the equivalent control $u_{1\text{eq}}$ given

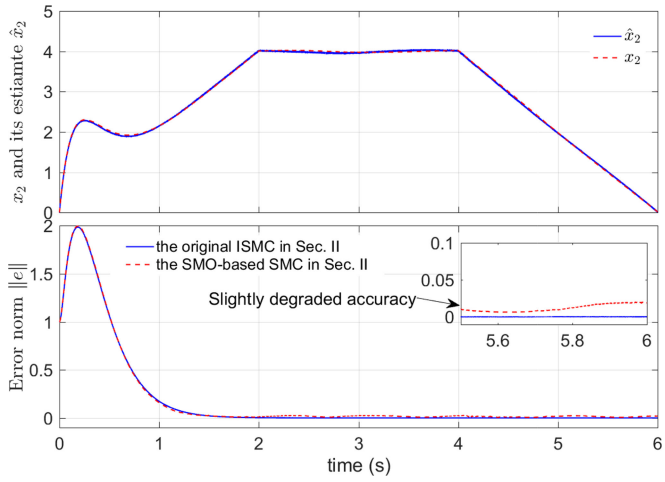

Fig. 2. Performance of the SMO-based ISMC in Section II.

by (17). Then, choose a new control law

$$u(t) = u_0(t) + u_{1\text{av}}(t) \tag{22}$$

where the nominal control u_0 is presented in (9). The principle of the above design is that the actual effect of the discontinuous u_1 is equal to the average of the control action, i.e., the equivalent control $u_{1\text{eq}}$, and the equivalence of u_1 is equal to the averaged control $u_{1\text{av}}$ measured by the low-pass filter with u_1 as its input in (21) (i.e., $u_{1\text{eq}} = u_{1\text{av}}$) [14, Sec. 7.4].

To answer questions "*How can the sliding mode be generated by the smoothed control* u_{1av}*?*" and "*Does* u_{1av} *still cancel out the perturbation h,*" it was suggested that the integral term z in (11) is redesigned as follows [14, Sec. 7]:

$$\dot{z} = -\frac{\partial s_0}{\partial \boldsymbol{e}}\left[\begin{array}{c}\bar{\boldsymbol{e}}_1 \\ \left[f_0(\boldsymbol{x}) - x_d^{(n)}\right] + g_0(\boldsymbol{x})u - g_0 u_1\end{array}\right] \tag{23}$$

with $z(0) = -s_0(\boldsymbol{e}(0))$. Applying the expressions of u in (22), s_0 in (6), u_0 in (9), and v under (7) to (23), one gets

$$\dot{z} = k_c s_0 + g_0(\boldsymbol{x})(u_1 - u_{1\text{av}}).$$

Applying the foregoing expression to (11), one obtains a modified integral sliding variable

$$s(t) = \int_0^t [k_c s_0 + g_0(\boldsymbol{x})(u_1 - u_{1\text{av}})]d\tau + s_0(\boldsymbol{e}(t)) - s_0(\boldsymbol{e}(0)). \tag{24}$$

Taking the time derivative of s in (24) and using (7) yields

$$\dot{s} = [f_0(\boldsymbol{x}) + v(\boldsymbol{x}, t)] + g_0(\boldsymbol{x})u + h(\boldsymbol{x}, t) + k_c s_0 + g_0(\boldsymbol{x})(u_1 - u_{1\text{av}}).$$

Applying (22) with (9) to the above equality, one obtains (14) with s being given by (24).

If the discontinuous control u_1 in (15) with s being given by (24) is applied to (14), the reaching law (16) is obtainable and the equivalent control $u_{1\text{eq}}$ is identical to (17) in Section II. Combining (17) with $u_{1\text{eq}} = u_{1\text{av}}$, one gets

$$u_{1\text{av}} = -h(\boldsymbol{x}, t)/g_0(\boldsymbol{x}) \tag{25}$$

such that the estimate of h is given by

$$\hat{h} = -g_0(\boldsymbol{x})u_{1\text{av}}. \tag{26}$$

However, due to the intrinsic discontinuity of u_1 in (15), the ideal result $\dot{s} = 0\ \forall t \geq 0$ is impossible to be obtained from (14) in practice. Without $\dot{s} = 0$, (17) is not obtainable such that (25) is also not obtainable, which implies the exact estimation of h by $\hat{h}$ in (26) is not realizable. Even if one has $\dot{s} = 0\ \forall t \geq 0$, setting $\dot{s} = 0$ in (24) yields the sliding mode dynamics

$$\dot{s}_0 + k_c s_0 + g_0(\boldsymbol{x})(u_1 - u_{1\text{av}}) = 0 \tag{27}$$

which implies s_0 converges to a neighborhood of 0 subject to g_0, μ, and k_c. Therefore, the tracking error $\boldsymbol{e}$ only converges to a compact set Ω_{c_e} subject to g_0, μ, k_c, and λ, where the size of Ω_{c_e} is not necessarily small since high-frequency switches in u_1 may result in a large discrepancy between u_1 and $u_{1\text{av}}$ even if the filtering constant μ in (21) is small.

To demonstrate the modified ISMC in this section, consider the same illustrative example with the same settings as that in Section II. The construction of the control law follows the steps in Section II except the filtering constant μ in (21) is set to be 0.1. Simulation trajectories are shown in Fig. 3, where the state vector $\boldsymbol{x}$ follows its desired signal $\boldsymbol{x}_d$ under a smooth control input u. However, although the sliding variable s still keeps near to 0 from $t = 0$, its time derivative $\dot{s}$ demonstrates serious chattering resulting in a large phase lag in the estimation of h even the setting of $\mu = 0.1$ is small. These results are consistent with the results of [14, Fig. 8.18]. Further decreasing μ is not suggested as it may introduce serious chattering at u.

Remark 3: For the system (1) driven by the modified ISMC law $u = u_0 + u_{1av}$ given by (22) with u_0 in (9), u_1 in (15), u_{1av} in (21), and s in (24), the performance of the reaching phase is identical to (16) by the original ISMC in Section II. Yet, the exact estimation of h in (5) is not realizable, and the performance of the sliding phase is degraded resulting in a compromise among chattering, tracking accuracy, and robustness, which are not consistent with the claim "*The concept of integral sliding mode can also be extended to construct a new type of perturbation estimator that solves the chattering problem without loss of robustness and control accuracy.*" in [14, Sec. 7].

IV. Global SMC

GSMC originated in [12] also aims to eliminate the reaching phase such that the sliding mode invariably exists and the invariance is guaranteed in an entire system response. In the GSMC, the integral term z of the sliding variable s in (11) is designed to satisfy the following conditions [30]: 1) $z(0) = -s_0(\boldsymbol{e}(0))$; 2) $z(t) \to 0$ as $t \to \infty$; 3) $\dot{z}(t)$ exists and is bounded. In the ISMC, if z is chosen as follows:

$$\dot{z} = -k_c z,\ z(0) = -s_0(\boldsymbol{e}(0)) \tag{28}$$

then the sliding variable s becomes

$$s(t) = s_0(\boldsymbol{e}(t)) - s_0(\boldsymbol{e}(0))e^{-k_c t} \tag{29}$$

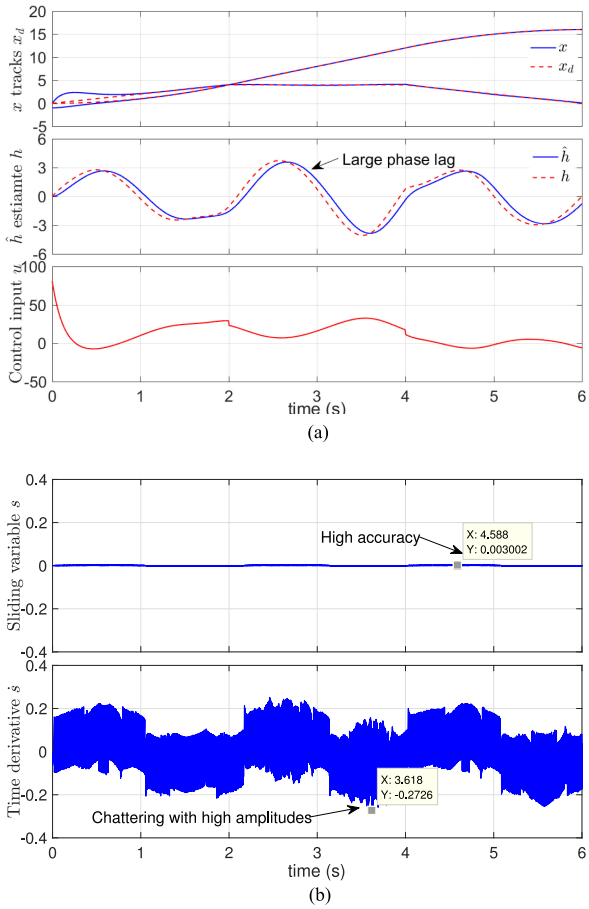

Fig. 3. Simulation trajectories by the modified ISMC in Section III. (a) Control and estimation performances. (b) Evaluations of s and $\dot{s}$.

which satisfies all the aforementioned conditions such that the resultant SMC belongs to a kind of GSMC.

Taking the time derivative of s in (29) and using (7) yields

$$\dot{s} = [f_0(\boldsymbol{x}) + v(\boldsymbol{x},t)] + g_0(\boldsymbol{x})u + h(\boldsymbol{x},t) - k_c z. \tag{30}$$

The control law is chosen as $u = u_0 + u_1$ in (8) with the nominal control u_0 in (9) and the discontinuous control u_1 in (15). Applying u_0 in (9) to (30), one obtains

$$\dot{s} = -k_c s + g_0(\boldsymbol{x})u_1 + h(\boldsymbol{x},t). \tag{31}$$

Applying u_1 in (15) to (31), one obtains

$$\begin{aligned} s\dot{s} &= -k_c s^2 + s\big(h(\boldsymbol{x},t) - g_0(\boldsymbol{x})\alpha \mathrm{sgn}(s)\big) \\ &\le -k_c s^2 + \big(|h(\boldsymbol{x},t)| - \bar{f} - \bar{d} - \eta\big)|s|\big). \end{aligned}$$

Noting (5) with Assumptions 1 and 2, the above result leads to an exponential reaching law [31]

$$s\dot{s} \le -k_c s^2 - \eta|s| \quad \forall \boldsymbol{x} \in \Omega_{c_x} \tag{32}$$

which is different form the standard reaching law (16). Combining (32) with $s(0) = 0$, one obtains $s(t) = 0\ \forall t \ge 0$. Setting $s = 0$ in (29), one obtains

$$s_0(\boldsymbol{e}(t)) = s_0(\boldsymbol{e}(0))e^{-k_c t} \tag{33}$$

which is exactly the solution of the ideal dynamics (10). Therefore, the performance of the GSMC at the sliding mode is the same as that of the ISMC in Section II.

Remark 4: The system (1) driven by the GSMC law $u = u_0 + u_1$ in (8) with u_0 in (9), u_1 in (15) and s in (29) ensures exponential convergence of the tracking error $\boldsymbol{e}$ to $\mathbf{0}$ during the reaching phase, which is the same as that by the original ISMC in Section II. Due to the exponential reaching law (32), the GSMC provides extra robustness against unanticipated perturbations compared with the ISMC in Section II [31].

V. High-Order Integral SMC

A more popular way of chattering attenuation in ISMC is to integrate with high-order SMC [10, Sec. 4]. Existing high-order ISMC methods require the information of $\dot{x}_n$ except the method of [23] with super twisting, where the perturbation h does not depend on the state vector $\boldsymbol{x}$ in [23]. It is worth noting that $\dot{x}_n$ is usually not accessible for measurement so that the requirement on $\dot{x}_n$ is not desirable in practice. The Lyapunov stability of the high-order SMC with super twisting was established in [33]. In this section, it is demonstrated that the high-order ISMC with super twisting [23] leads to a stability condition that is usually infeasible in theory if h depends on $\boldsymbol{x}$.

Recall the reduced-order system (7) driven by the control law $u = u_0 + u_1$ in (8) with u_0 in (9). The following additional assumptions are required to proceed the control design.

Assumption 4: Δf and Δg are continuously differentiable.

Assumption 5: $\dot{d}$ is globally bounded, i.e., there is a constant $\bar{d}_d \in \mathbb{R}^+$ such that $|\dot{d}(t)| \le \bar{d}_d\ \forall t \ge 0$.

The discontinuous control u_1 in (8) of Section II is replaced by a super-twisting algorithm [23]

$$\begin{cases} u_1 = (-k_s\sqrt{|s|}\mathrm{sgn}(s) + \vartheta)/g_0(\boldsymbol{x}) \\ \dot{\vartheta} = -\alpha \mathrm{sgn}(s) \end{cases} \tag{34}$$

with $\vartheta(0) = 0$, $k_s = 1.5\sqrt{\bar{h}_d}$, and $\alpha = 1.1\bar{h}_d$, where s is given by (13), $\vartheta \in \mathbb{R}$ is an auxiliary variable, and $\bar{h}_d \in \mathbb{R}^+$ is a upper bound of $\dot{h}$ that satisfies $|\dot{h}(\boldsymbol{x},t)| \le \bar{h}_d$, $\forall \boldsymbol{x} \in \Omega_{c_x}$. Applying (34) to (14) yields the closed-loop dynamics

$$\begin{cases} s = -k_s\sqrt{|s|}\mathrm{sgn}(s) + \vartheta + h(\boldsymbol{x},t) \\ \dot{\vartheta} = -\alpha \mathrm{sgn}(s). \end{cases} \tag{35}$$

It follows from [23] that (35) guarantees $s(t) = 0\ \forall t \ge 0$ and $\vartheta(t) = -h(\boldsymbol{x}(t),t)$ after a finite time. Thus, the tracking error $\boldsymbol{e}$ exponentially converges to $\mathbf{0}$ and the estimate $\hat{h} := -\vartheta$ exactly follows the perturbation h after a finite time.

The intention of introducing Assumptions 4 and 5 is to ensure the existence of the upper bound $\bar{h}_d$. Yet, $\bar{h}_d$ still may not exist under the additional two assumptions. To clarify this claim, the time derivative of h given by (5) is derived as follows:

$$\dot{h}(\boldsymbol{x},t) = \frac{\partial \Delta f}{\partial \boldsymbol{x}} \begin{bmatrix} \bar{\boldsymbol{x}}_1 \\ [f(\boldsymbol{x}) + g(\boldsymbol{x})u + d(t)] \end{bmatrix} + \dot{d}(t)$$

with $\bar{\boldsymbol{x}}_1 := [x_2, x_3, \cdots, x_n]^T$. Thus, one obtains

$$\dot{h}(\boldsymbol{x},t) = f_a(\boldsymbol{x}) + f_b(\boldsymbol{x})[f(\boldsymbol{x}) + g(\boldsymbol{x})u + d(t)] + \dot{d}(t).$$

where $f_a(\boldsymbol{x}) := \sum_{i=1}^{n-1} \frac{\partial \Delta f}{\partial x_i} x_{i+1}$ and $f_b(\boldsymbol{x}) := \frac{\partial \Delta f}{\partial x_n}$. Applying $u = u_0 + u_1$ in (8) to the above result leads to

$$\dot{h}(\boldsymbol{x},t) = f_a(\boldsymbol{x}) + f_b(\boldsymbol{x})(f(\boldsymbol{x}) + g(\boldsymbol{x})u_0 + d(t)) + \dot{d}(t) + f_b(\boldsymbol{x})g(\boldsymbol{x})u_1 \le \bar{h}_d. \quad (36)$$

Intuitionally, it follows from (36) that $\bar{h}_d$ is hard to be determined as u_1 depends on $\bar{h}_d$ via k_s and α in (34) so that a large $\bar{h}_d$ also leads to a large amplitude at the left side of "$\le$" in (36). The detailed analysis is given as follows.

Noting Assumptions 1 and 4, let $c_a := \max_{\boldsymbol{x}\in\Omega_{cx}} \{|f_a(\boldsymbol{x})|\} \in \mathbb{R}^+$, $c_b := \max_{\boldsymbol{x}\in\Omega_{cx}} \{|f_b(\boldsymbol{x})|\} \in \mathbb{R}^+$ and $c_{u_0} := \max_{\boldsymbol{x}\in\Omega_{cx}} \{|g_0(\boldsymbol{x})u_0|\} \in \mathbb{R}^+$. Applying the above definitions to (36) and noting Assumptions 1, 2, and 5 and $g(\boldsymbol{x}) = g_0(\boldsymbol{x})$, one gets

$$\dot{h}(\boldsymbol{x},t) \le c_a + c_b(\bar{f} + \bar{d} + c_{u_0}) + \dot{\bar{d}}_d + f_b(\boldsymbol{x})g_0(\boldsymbol{x})u_1.$$

Applying $k_s = 1.5\sqrt{\bar{h}_d}$ and $\alpha = 1.1\bar{h}_d$ to (34), one obtains

$$g_0(\boldsymbol{x})u_1 = -1.5\sqrt{\bar{h}_d|s|}\,\mathrm{sgn}(s) - 1.1\bar{h}_d \int_0^t \mathrm{sgn}(s(\tau))d\tau.$$

Combining with the above two results, one obtains

$$\dot{h}(\boldsymbol{x},t) \le c_a + c_b(\bar{f} + \bar{d} + c_{u_0}) + \dot{\bar{d}}_d + 1.5c_b\sqrt{\bar{h}_d|s|} - 1.1\bar{h}_d f_b(\boldsymbol{x}) \int_0^t \mathrm{sgn}(s(\tau))d\tau$$

where the upper bound at the right size of "$\le$" is not conservative as it is the frequent case that upper bounds are positive.

The above inequality implies the selection of $\bar{h}_d$ has to satisfy

$$\bar{h}_d\left(1 + 1.1f_b(\boldsymbol{x}) \int_0^t \mathrm{sgn}(s(\tau))d\tau\right) \ge c_a + c_b(\bar{f} + \bar{d} + c_{u_0}) + \dot{\bar{d}}_d + 1.5c_b\sqrt{\bar{h}_d|s|}.$$

As all items at the right side of the above inequality are positive, a necessary condition for the existence of $\bar{h}_d$ is

$$f_b(\boldsymbol{x}) \int_0^t \mathrm{sgn}(s(\tau))d\tau \ge -1/1.1 \quad (37)$$

which is very stringent since it requires the left of "$\le$" always being equal to or larger than $-1/1.1$. At an extreme case that (37) is satisfied, let $c_f := \min_{\boldsymbol{x}\in\Omega_{cx}} \{1+1.1f_b(\boldsymbol{x}) \int_0^t \mathrm{sgn}(s(\tau))d\tau\} \in \mathbb{R}^+$, $c_g := \max_{\boldsymbol{x}\in\Omega_{cx}} \{1.5c_b\sqrt{|s|}\} \in \mathbb{R}^+$ and $c_h := c_a + c_b(\bar{f} + \bar{d} + c_{u_0}) + \dot{\bar{d}}_d$. Then, one obtains

$$\left(\sqrt{\bar{h}_d}\right)^2 - (c_g/c_f)\sqrt{\bar{h}_d} \ge c_h/c_f.$$

Completing the square at the left side of the above inequality, one gets its equivalent expression

$$\left(\sqrt{\bar{h}_d} - c_g/(2c_f)\right)^2 \ge c_h/c_f + c_g^2/(2c_f)^2$$

which is also equivalent to

$$\bar{h}_d \ge \left[\sqrt{c_h/c_f + c_g^2/(2c_f)^2} + c_g/(2c_f)\right]^2 \quad (38)$$

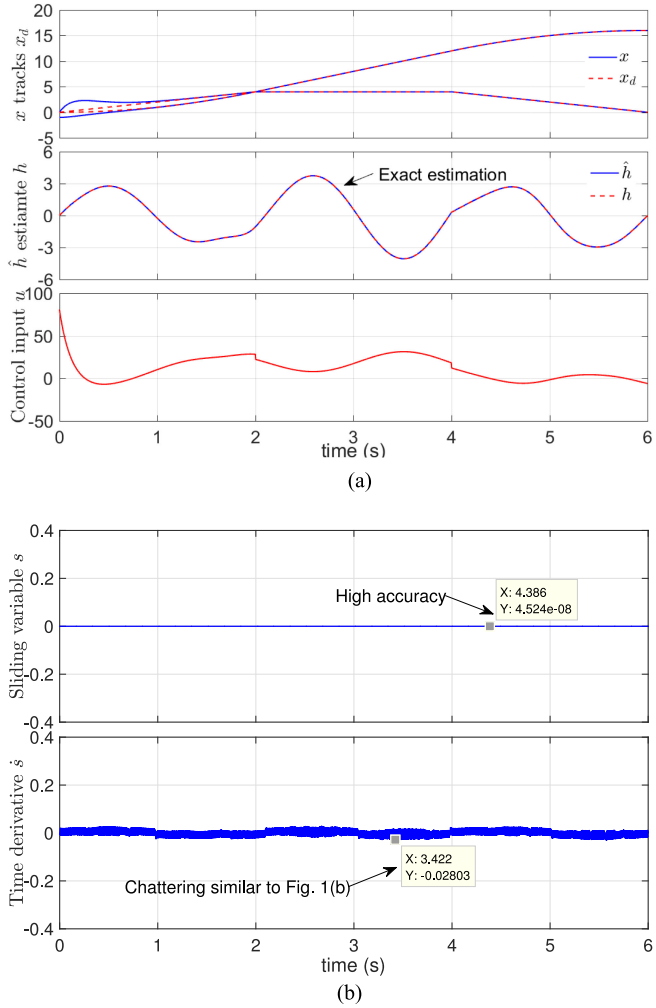

Fig. 4. Simulation trajectories by the high-order ISMC in Section V. (a) Control and estimation performances. (b) Evaluations of s and $\dot{s}$.

where the right side of "$\ge$" is usually extremely larger than $(\bar{f} + \bar{d})$, the upper bound of $h(\boldsymbol{x},t)$ for the ISMC in Section II.

To illustrate the high-order ISMC with super twisting in this section, consider the same illustrative example with the same settings as that in Section II. The construction of the control law follows the steps in Section II except the upper bound $\bar{h}_d$ in (34) is set as 20. Simulation trajectories are depicted in Fig. 4. Despite the limitations discussed in [26], the super-twisting high-order ISMC with the larger switching gain α achieves high tracking and estimation accuracy under a smooth control input u, which is not consistent with the above analysis. The chattering at $\dot{s}$ is similar to that of the original ISMC in Section II.

Remark 5: For the system (1) under the super-twisting high-order ISMC law $u = u_0 + u_1$ in (8) with u_0 in (9), u_1 in (34), and s in (13), exponential convergence of the tracking error $\boldsymbol{e}$ and an exact estimation of the perturbation h are shown under the stability condition (37) with (38) that is usually infeasible in theory. However, the superior tracking and estimation performances shown in Fig. 4 differ from the theoretical analysis, which implies the selection of the gains k_s and α in (34) may

be improper and further studies based on advanced high-order SMC techniques such as [32] is still desirable.

VI. Suggested Chattering Reduction Scheme

To resolve the chattering problem, we suggest to utilize the filtering solution in Section III without the integral sliding variable modification in (23), i.e., we use the control law

$$u(t) = u_0(t) + u_{1\text{av}}(t) \tag{39}$$

where the nominal control u_0 is given by (9), and the averaged control $u_{1\text{av}}$ is generated by (21) with the discontinuous control u_1 in (15) as its input. The sliding variable s is given by (29), corresponding to the suggested GSMC design. This suggestion is well supported by the equivalent control principle [14, Sec. 7.4]: the equivalence of u_1 is equal to $u_{1\text{av}}$ as long as the filtering bandwidth of (18) covers the frequency spectrum of the perturbation h. Substituting (39) with (9) to (30), one obtains

$$\dot{s} = -k_c s + g_0(\boldsymbol{x})u_{1\text{av}} + h(\boldsymbol{x}, t) \tag{40}$$

which differs from (31). Noting the continuity of $u_{1\text{av}}$ and $s(t) = 0\ \forall t \geq 0$, the ideal result $\dot{s} = 0\ \forall t \geq 0$ is possible from (40) in practice. Setting $\dot{s} = s = 0$ in (40) yields [14, Sec. 7]

$$u_{1\text{eq}} = u_{1\text{av}} = -h(\boldsymbol{x}, t)/g_0(\boldsymbol{x}). \tag{41}$$

Hence, if the filtering constant μ in (21) is chosen to be small enough such that the filtering bandwidth of (21) covers the frequency spectrum of h, $\hat{h}$ in (26) provides an exact estimation of h according to (41). In Section II, it is unreasonable to let $u_1 = u_{1\text{eq}}$ as u_1 includes high-frequency contents that may not present in $u_{1\text{eq}}$. Instead, it is more reasonable to have $u_{1\text{av}} = u_{1\text{eq}}$ as high frequency contents are filtered out in $u_{1\text{av}}$. Consequently, it is reasonable to expect $u_{1\text{av}}$ performs similarly to u_1 with respect to tracking accuracy under reduced chattering.

In the above discussions, we assume $\Delta g(\boldsymbol{x}) = 0$ for clear presentation. Now, the suggested GSMC design is extended to the case with $\Delta g(\boldsymbol{x}) \neq 0$. Let $\Delta g(\boldsymbol{x}) \neq 0$ in (1) such that the reduced-order system (7) becomes

$$\begin{aligned}\dot{s}_0 = {} & [f_0(\boldsymbol{x}) + v(\boldsymbol{x}, t)] + \Delta f(\boldsymbol{x}) + d(t) \\ & + [g_0(\boldsymbol{x}) + \Delta g(\boldsymbol{x})]u.\end{aligned} \tag{42}$$

Applying the control law (8) with (9) to (42), one obtains

$$\dot{s}_0 = -k_c s_0 + g(\boldsymbol{x})(h(\boldsymbol{x}, t) + u_1) \tag{43}$$

where the perturbation h is redefined by

$$h(\boldsymbol{x}, t) := [\Delta f(\boldsymbol{x}) + \Delta g(\boldsymbol{x})u_0 + d(t)]/g(\boldsymbol{x}). \tag{44}$$

Taking the time derivative of s in (29) along (43) yields

$$\dot{s} = -k_c s + g(\boldsymbol{x})(h(\boldsymbol{x}, t) + u_1). \tag{45}$$

Choose the discontinuous control

$$u_1 = -\alpha \text{sgn}(s),\ \alpha \geq (\bar{f} + \bar{g}\bar{u}_0 + \bar{d} + \eta)/\underline{g} \tag{46}$$

with $\bar{u}_0 := \max_{\boldsymbol{x} \in \Omega_{cx}} \{u_0\}$. Applying (46) to (45) yields

$$\begin{aligned} s\dot{s} &= -k_c s^2 + sg(\boldsymbol{x})(h(\boldsymbol{x}, t) - \alpha \text{sgn}(s)) \\ &\leq -k_c s^2 + g(\boldsymbol{x})\big(|h(\boldsymbol{x}, t)| - (\bar{f} + \bar{g}\bar{u}_0 + \bar{d} + \eta)/\underline{g}\big)|s|. \end{aligned}$$

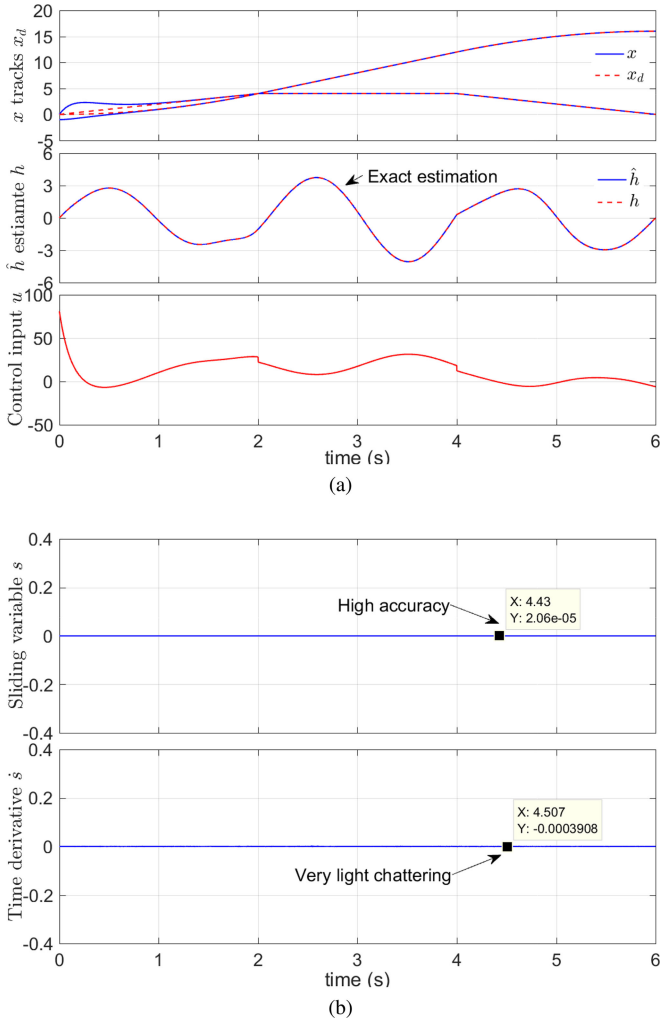

Fig. 5. Control trajectories by the suggested GSMC with $\Delta g(\boldsymbol{x}) = 0$. (a) Control and estimation performances. (b) Evaluations of s and $\dot{s}$.

Noting (44) and Assumptions 1 and 2, one obtains the exponential reaching law (32). Following the same derivations as the case with $\Delta g(\boldsymbol{x}) = 0$, one gets $\boldsymbol{e} \to \boldsymbol{0}$ exponentially. To tackle the chattering problem, the GSMC law is chosen as (39), where u_0 is given by (9), $u_{1\text{av}}$ is generated by (21) with u_1 in (46) as its input, and s is given by (29). Then, one obtains

$$\dot{s} = -k_c s + g(\boldsymbol{x})(h(\boldsymbol{x}, t) + u_{1\text{av}}) \tag{47}$$

so that an exact estimation of h in (44) is obtained by

$$\hat{h} = -u_{1\text{av}} \tag{48}$$

as in the case of $\Delta g(\boldsymbol{x}) = 0$. Note that to handle the uncertainty $\Delta g(\boldsymbol{x})$ in the control gain function $g(\boldsymbol{x})$, the switching gain α in (46) is designed to be much larger than that of the case with an exactly known $g(\boldsymbol{x})$ in (15).

To illustrate the suggested GSMC under the case of $\Delta g(\boldsymbol{x}) = 0$, consider the same illustrative example with the same settings and controller construction as that in Section II. Simulation trajectories by the suggested GSMC are depicted in Fig. 5, where an exact estimation of h in (5) by $\hat{h}$ in (26) is achieved without

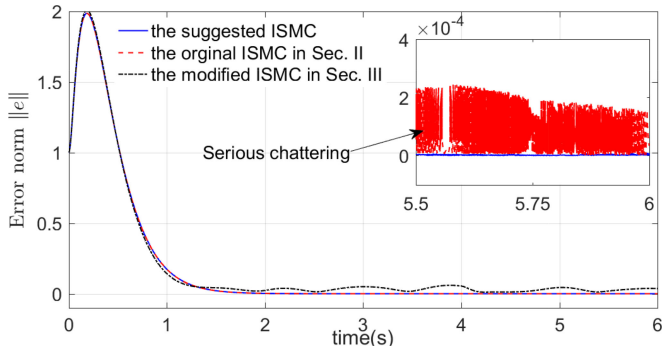

Fig. 6. Tracking error comparison of various ISMC designs.

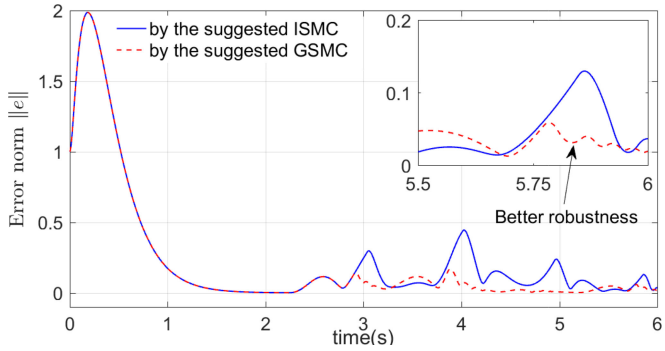

Fig. 7. Tracking error comparison of suggested control designs.

any phase lag, an exact tracking of $\boldsymbol{x}_d$ by $\boldsymbol{x}$ is obtained under a smooth control input u without the tradeoff between chattering reduction and tracking accuracy, and the chattering at $\dot{s}$ is reduced to be much lighter than that by the super-twisting high-order ISMC in Fig. 4. A tracking error comparison of different ISMC designs is presented in Fig. 6, where the original ISMC in Section II exhibits chattering due to the intrinsic discontinuity of the control input u, the modified ISMC in Section III gets the worst tracking accuracy due to the imperfect estimation of h [see Fig. 3(a)] and the degraded performance of the sliding phase [see (27)], and the suggested GSMC achieves the highest tracking accuracy without chattering.

To validate the superiority of the suggested GSMC, consider the same illustrative example with the same settings as that in Section II except the amplitude of the external disturbance d in (1) is increased from 3 to 5 after $t = 2$ s. The suggested ISMC is obtained by applying s given by (13) to replace s given by (29) in the suggested GSMC. A tracking error comparison between the suggested ISMC and GSMC designs is presented in Fig. 7, where the exact estimation of h in (5) by $\hat{h}$ in (26) loses after $t = 2$ s for both the controllers due to the unanticipated large d, and the suggested GSMC exhibits better robustness against d reflected by higher tracking accuracy after $t = 2$ s.

To illustrate the suggested GSMC under the case of $\Delta g(\boldsymbol{x}) \neq 0$, consider the same illustrative example with the same settings as Section II except $m = m_0 + 1.5\sin(|x_2|t)$ implying $\Delta f(\boldsymbol{x}) = (1.2 + 0.2\sin(|x_2|t)x_2|x_2|/(3 + 1.5\sin(|x_2|t)$ $-1.2x_2|x_2|/3$ and $\Delta g(\boldsymbol{x}) = 1/(3 + 1.5\sin(|x_2|t) - 1/3$. The construction of the control law is the same as that of the case with $\Delta g(\boldsymbol{x}) = 0$ except the switching gain α is increased from 13 to 19. With the definitions of h in (44), u_0 in (9), and v under (7), one gets that the piecewise continuity of $\ddot{x}_d$ results in two piecewise points of h in (44) at $t = 2$ and 4 s. Simulation trajectories of this case depicted in Fig. 8 are very similar to those in Fig. 5 except light oscillations exist in $\hat{h}$ and $\dot{s}$ near $t = 2$ and 4 s due to the piecewise points of h at $t = 2$ and 4 s.

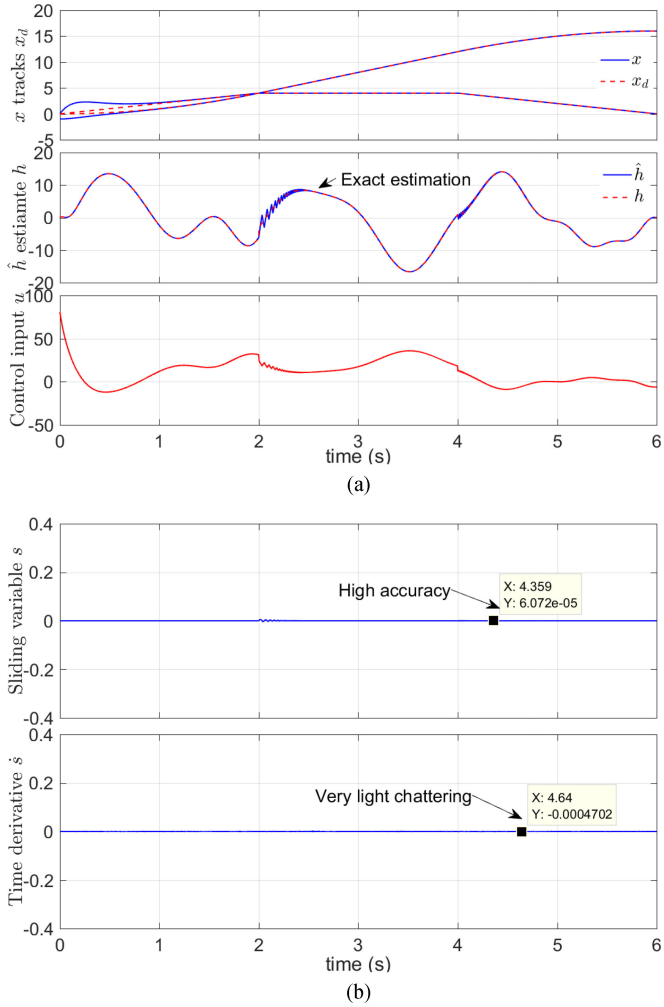

Fig. 8. Simulation trajectories by the suggested GSMC with $\Delta g(\boldsymbol{x}) \neq 0$. (a) Control and estimation performances. (b) Evaluations of s and $\dot{s}$.

Remark 6: The suggested ISMC/GSMC design significantly alleviates the compromise among chattering, tracking accuracy, and robustness in SMC. Compared with the high-order ISMC in Section V, the distinctive feature of the suggested design is that the perturbation h in (5)/(44) is exactly estimated by a much simpler control scheme. One major deficiency of the suggested design is that the setting of the filtering constant μ in (21) is subject to the frequency spectrum of h such that chattering may not be well attenuated when μ needs to be very small. Note that the transient occurs if $h(0) \neq 0$ as $u_{1\text{av}}(0) = 0$ in (21).

VII. Conclusion

This study has discussed several crucial problems in ISMC, where conclusions are drawn as follows:

1) The modification of the integral sliding variable degrades the performance of the sliding mode.
2) ISMC belongs to a kind of GSMC.
3) The super-twisting high-order ISMC usually results in a stability condition that is infeasible in theory.

The low-pass filtering solution without the modification of the integral sliding variable is suggested for chattering attenuation in ISMC. Comprehensive simulations have validated the arguments of study and have demonstrated a superior performance of the suggested ISMC design in terms of chattering attenuation, trajectory tracking, and disturbance estimation. The application of the suggested ISMC to handle perturbations in composite learning control [34] would be interesting for further study.

References

[1] A. Sabanovic, "Variable structure systems with sliding modes in motion control-A survey," *IEEE Trans. Ind. Inf.*, vol. 7, pp. 212–223, May 2011.

[2] A. Hace and M. Franc, "FPGA implementation of sliding-mode-control algorithm for scaled bilateral teleoperation," *IEEE Trans. Ind. Inf.*, vol. 9, no. 3, pp. 1291–1300, Aug. 2013.

[3] F. F. M. El-Sousy, "Adaptive dynamic sliding-mode control system using recurrent RBFN for high-performance induction motor servo drive," *IEEE Trans. Ind. Inf.*, vol. 9, no. 4, pp. 1922–1936, Nov. 2013.

[4] J. R. Dominguez, A. Navarrete, M. A. Meza, A. G. Loukianov, and J. Canedo, "Digital sliding-mode sensorless control for surface-mounted PMSM," *IEEE Trans. Ind. Inf.*, vol. 10, no. 1, pp. 137–151, Feb. 2014.

[5] P. Ignaciuk, "Nonlinear inventory control with discrete sliding modes in systems with uncertain delay" *IEEE Trans. Ind. Inf.*, vol. 10, no. 1, pp. 559–568, Feb. 2014.

[6] Q. S. Xu, "Digital sliding-mode control of piezoelectric micropositioning system based on input-output model," *IEEE Trans. Ind. Electron.*, vol. 61, no. 10, pp. 5517–5526, Oct. 2014.

[7] J. Yang, J. Y. Su, S. H. Li, and X. H. Yu, "High-order mismatched disturbance compensation for motion control systems via a continuous dynamic sliding-mode approach," *IEEE Trans. Ind. Inf.*, vol. 10, no. 1, pp. 604–614, Feb. 2014.

[8] C. C. Chen, S. S. D. Xu, and Y. W. Liang, "Study of nonlinear integral sliding mode fault-tolerant control," *IEEE/ASME Trans. Mechatron.*, vol. 21, no. 2, pp. 1160–1168, Apr. 2016.

[9] S. Biricik and H. Komurcugil, "Optimized sliding node control to maximize existence region for single-phase dynamic voltage restorers," *IEEE Trans. Ind. Inf.*, vol. 12, no. 14, pp. 1486–1497, Aug. 2016.

[10] Y. Shtessel, C. Edwards, L. Fridman, and A. Levant, *Sliding Mode Control and Observation*. New York, NY, USA: Springer, 2014.

[11] J. Y. Hung, W. Gao, and J. C. Hung, "Variable structure control: A survey," *IEEE Trans. Ind. Electron.*, vol. 40, no. 1, pp. 2–22, Feb. 1993.

[12] Y. S. Lu and J. S. Chen, "Design of a global sliding-mode controller for a motor drive with bounded control," *Int. J. Control*, vol. 62, no. 5, pp. 1001–1019, Nov. 1995.

[13] V. Utkin and J. Shi, "Integral sliding mode in systems operating under uncertainty conditions," in *Proc. IEEE Conf. Decision Control*, Kobe, Japan, 1996, pp. 4591–4596.

[14] V. Utkin, J. Guldner, and J. Shi, *Sliding Mode Control in Electro-Mechanical Systems*, 2nd ed. Boca Raton, FL, USA: CRC Press, 2009.

[15] J. Shi, H. Liu, and N. Bajcinca, "Robust control of robotic manipulators based on integral sliding mode," *Int. J. Control*, vol. 81, no. 10, pp. 1537–1548, Oct. 2008.

[16] J. Komsta, N. van Oijen, and P. Antoszkiewicz, "Integral sliding mode compensator for load pressure control of diecushion cylinder drive," *Control Eng. Prac.*, vol. 21, no. 5, pp. 708–718, May. 2013.

[17] M. Das and C. Mahanta, "Optimal second order sliding mode control for nonlinear uncertain systems," *ISA Trans.*, vol. 53, no. 4, pp. 1191–1198, Jul. 2014.

[18] A. Ferrara and G. P. Incremona, "Design of an integral suboptimal second-order sliding mode controller for the robust motion control of robot manipulators," *IEEE Trans. Control Syst. Technol.*, vol. 23, no. 6, pp. 2316–2325, Nov. 2015.

[19] H. Rios, S. Kamal, L. M. Fridman, and A. Zolghadri, "Fault tolerant control allocation via continuous integral sliding-modes: A HOSM-observer approach," *Automatica*, vol. 51, pp. 318–325, Jan. 2015.

[20] P. R. Kumar, A. Chalanga, and B. Bandyopadhyay, "Smooth integral sliding mode controller for the position control of Stewart platform," *ISA Trans.*, vol. 58, pp. 543–551, Sep. 2015.

[21] P. M. Tiwari, S. Janardhanan, and M. un Nabi, "Rigid spacecraft attitude control using adaptive integral second order sliding mode," *Aerosp. Sci. Technol.*, vol. 42, pp. 50–57, Apr./May 2015.

[22] M. Taleb, F. Plestan, and B. Bououlid, "An adaptive solution for robust control based on integral high-order sliding mode concept," *Int. J. Robust Nonlinear Control*, vol. 25, pp. 1201–1213, May 2015.

[23] A. Chalanga, S. Kamal, and B. Bandyopadhyay, "A new algorithm for continuous sliding mode control with implementation to industrial emulator setup," *IEEE/ASME Trans. Mechatronics*, vol. 20, no. 5, pp. 2194–2204, Oct. 2015.

[24] A. Levant, "Higher-order sliding modes, differentiation and output-feedback control," *Int. J. Control*, vol. 76, no. 9, pp. 924–941, 2003.

[25] V. Utkin, *Sliding Modes in Control and Optimization*. Berlin, Germany: Springer, 1992.

[26] V. Utkin, "Discussion aspects of high-order sliding mode control," *IEEE Trans. Autom. Control*, vol. 61, no. 3, pp. 829–833, Mar. 2016.

[27] B. Xian, D. M. Dawson, M. S. de Queiroz, and J. Chen, "A continuous asymptotic tracking control strategy for uncertain nonlinear systems," *IEEE Trans. Autom. Control*, vol. 49, no. 7, pp. 1206–1211, Jul. 2004.

[28] J.-J. E. Slotine and W. Li, *Applied Nonlinear Control*. Englewood Cliffs, NJ, USA: Prentice-Hall, 1991.

[29] R. J. Wai, "Adaptive sliding-mode control for induction servomotor drive," *IEE Proc. Electr. Power Appl.*, vol. 147, no. 6, pp. 553–562, Nov. 2000.

[30] H. S. Choi, Y. H. Park, Y. S. Cho, and M. H. Lee, "Global sliding-mode control—Improved design for a brushless DC motor," *IEEE Control Syst. Mag.*, vol. 21, no. 3, pp. 27–35, Jun. 2001.

[31] W. B. Gao and J. C. Hung, "Variable structure control of nonlinear systems: A new approach," *IEEE Trans. Ind. Electron.*, vol. 40, no. 1, pp. 45–55, Feb. 1993.

[32] I. Castillo, L. Fridman, and J. A. Moreno, "Super-twisting algorithm in presence of time and state dependent perturbations," *Int. J. Control*, to be published.

[33] R. Seeber and M. Horn, "Stability proof for a well-established super-twisting parameter setting," *Automatica*, vol. 84, pp. 241–243, Oct. 2017.

[34] Y. P. Pan and H. Y. Yu, "Composite learning from adaptive dynamic surface control," *IEEE Trans. Autom. Control*, vol. 61, no. 9, pp. 2603–2609, Sep. 2016.

Yongping Pan (M'14) received the Ph.D. degree in control theory and control engineering from the South China University of Technology, Guangzhou, China, in 2011.

He was a Control Engineer with the Santak Electronic Co., Ltd., US Eaton Group, Shenzhen, China, and the U.S. Light Engineering Co., Ltd., Guangzhou, from 2007 to 2008. From 2011 to 2013, he was a Research Fellow with the School of Electrical and Electronic Engineering, Nanyang Technological University, Singapore. He is currently a Senior Research Fellow with the Department of Biomedical Engineering, National University of Singapore, Singapore. His research interests include nonlinear and adaptive control, neural networks and learning systems, and their applications to compliant robots. He has authored or coauthored more than 80 peer-reviewed academic papers, including more than 60 in refereed journals.

Dr. Pan has been invited an Associate Editor or Editorial Board Member of numerous refereed journals and has served on a number of conference organizing committees. He has also served as a Reviewer for more than 50 refereed journals.

Chenguang Yang (M'10–SM'16) received the B.Eng. degree in measurement and control from Northwestern Polytechnical University, Xi'an, China, in 2005, and the Ph.D. degree in control engineering from the National University of Singapore, Singapore, in 2010.

He received postdoctoral training at the Imperial College London, London, U.K. Currently, he is with the Zienkiewicz Centre for Computational Engineering, Swansea University, U.K. His research interests include robotics, automation, and computational intelligence.

Dr. Yang received the Best Paper Award from the IEEE TRANSACTIONS ON ROBOTICS in 2011.

Lin Pan received the M.Sc. degree in applied mathematics from the Wuhan University of Technology, Wuhan, China, in 2007 and the Ph.D. degree in control engineering from the Donghua University, Shanghai, China, in 2010, with the Sino-German joint Ph.D. of the University of Hagen, Hagen, Germany.

He was a Postdoctoral Trainee with the King Saud University, Riyadh, Saudi Arabia. He was with the SnT-Interdisciplinary Centre for Security, Reliability and Trust, University of Luxembourg, Luxembourg, as a Marie Curie Fellow and Senior Researcher during 2013–2014. He is currently a Professor with the School of Logistics Engineering, Wuhan University of Technology, Wuhan, China. His current research interests include control of large-scale port wind farms, shore-to-ship power supply system in port, complex dynamic network system, and multiagent systems.

Haoyong Yu (M'10) received the Ph.D. degree in mechanical engineering from Massachusetts Institute of Technology, Cambridge, MA, USA, in 2002.

He was a Principal Member of Technical Staff at DSO National Laboratories, Singapore, until 2002. He is currently an Associate Professor with the Department of Biomedical Engineering and a Principal Investigator of the Singapore Institute of Neurotechnology, National University of Singapore, Singapore. His areas of research include medical robotics, rehabilitation engineering and assistive technologies, system dynamics and control.

Dr. Yu received the Outstanding Poster Award at the IEEE Life Sciences Grand Challenges Conference 2013. He has served on a number of IEEE conference organizing committees.